

# Comparative study of the proton- $\eta$ and proton- $\eta'$ interactions via the $pp$ and $p$ -meson invariant mass distributions measured at COSY-11

P. Klaja for the COSY-11 collaboration

*Nuclear Physics Department, Jagellonian University, 30-059 Cracow, Poland  
Institut für Kernphysik, Forschungszentrum Jülich, 52425 Jülich, Germany*

**Abstract.** The COSY-11 collaboration has performed measurements of  $pp \rightarrow pp\eta$  and  $pp \rightarrow pp\eta'$  reactions at the excess energy  $Q = 15.5$  MeV. The determined  $pp$  and  $p$ -meson invariant mass distributions are used for comparative study of the interaction within *proton – meson* system. Presently we are finishing the analysis of the  $pp \rightarrow pp\eta'$  reaction and the resulted preliminary invariant mass distributions will be presented and compared to the theoretical predictions and to the corresponding spectra for the  $pp\eta$  system.

**Keywords:** meson production,  $\eta$  and  $\eta'$  mesons, meson-nucleon interaction

**PACS:** 13.60.Le, 13.75.-n, 14.40.-n, 25.40.-h

## INTRODUCTION

The COSY-11 collaboration continues the comparative study of interaction of the  $\eta$  and  $\eta'$  mesons with protons. To perform that studies the  $pp \rightarrow pp\eta$  and  $pp \rightarrow pp\eta'$  reactions were measured at beam momentum of 2.0259 GeV/c and 3.257 GeV/c, respectively. Those momenta correspond to the excess energy  $Q = 15.5$  MeV.

First part of investigations, namely the study of the proton- $\eta$  interaction is finished. The completed evaluation of the high-statistics measurement of the  $pp \rightarrow pp\eta$  reaction was published in reference [1]. Presently, the analysis of the  $pp \rightarrow pp\eta'$  reaction is in progress. It is carried out in a similar way as it has been done for the  $pp\eta$  system. The determined  $pp$  and  $p$ -meson invariant mass distributions will be used for comparative study of the interaction within *proton – meson* system.

Near the kinematical threshold measurements of nucleon-nucleon collisions allow to study the particles production with the dominant contribution from one partial wave only. Also, the interaction between particles in the near threshold collisions determines strongly the dependance of the total cross section as a function of the centre-of-mass excess energy. The excitation functions for the  $pp \rightarrow pp\eta'$  [2, 3] and  $pp \rightarrow pp\eta$  [3, 4, 5, 6, 7] reactions are presented in the figure 1. Comparing the data to the arbitrarily normalized phase-space integral reveals that proton-proton FSI enhances the total cross section by more than one order of magnitude for low energies. Also, one recognizes that in case of the  $\eta'$  meson production the data are described well assuming that the on-shell proton-proton amplitude exclusively determines the phase-space population. This indicates that the proton- $\eta'$  interaction is too small to manifest itself in the excitation

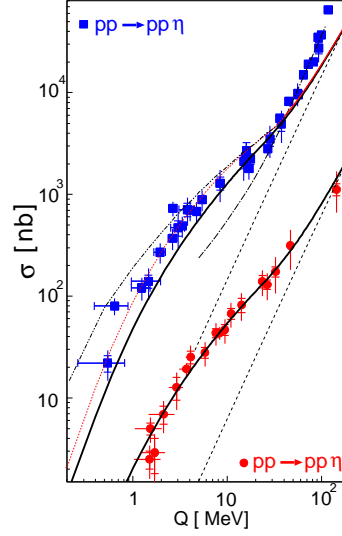


**FIGURE 1.** Total cross section for reactions  $pp \rightarrow pp\eta'$  (circles) and  $pp \rightarrow pp\eta$  (squares) as a function of the centre-of-mass excess energy. Data are from references [2, 3, 4, 5, 6, 7]. The dashed lines indicate a phase-space integral normalized arbitrarily. The solid lines depict the calculations with inclusion of the  $^1S_0$  proton-proton strong and Coulomb interactions. Additional inclusion of the proton- $\eta$  interaction is showed by the dotted line [8]. The dashed-dotted line indicates the energy dependence taking into account the contribution from the  $^3P_0 \rightarrow ^1S_0s$ ,  $^1S_0 \rightarrow ^3P_0s$  and  $^1D_2 \rightarrow ^3P_2s$  transitions [9]. The results of the  $^3P_0 \rightarrow ^1S_0s$  transition with the full treatment of the three-body effects are presented by the dashed-double-dotted line [10].

function within the presently achieved statistical uncertainty.

## INTERACTION WITHIN $pp\eta$ SYSTEM

The interaction between particles depends on their relative momenta or equivalently on the invariant masses of the two-particles subsystems. It should manifest itself as modification of the phase-space abundance in kinematical regions where particles have small relative velocities. For a three particle system only two invariant masses of three subsystems are independent and therefore the whole accessible information about the final state interaction can be showed in the Dalitz plot. One can also use the projection of the phase-space distribution onto the invariant masses of proton-proton or proton-meson subsystems [1].

In the case of the  $pp \rightarrow pp\eta$  reaction qualitative phenomenological analysis of the determined differential invariant proton-proton and proton- $\eta$  mass distributions revealed an enhancement of the population density at the kinematical region corresponding to the small proton- $\eta$  momentum. The proton-proton and proton- $\eta$  invariant mass distributions are presented in figure 2. One can easily see that mentioned effect occurs to be too large to be described by the inclusion of the on-shell proton-proton and proton- $\eta$  FSI. In fact a better description is achieved when contributions from higher partial waves or off-shell effects of the proton-proton potential are taken into account. These calculations compared to the experimentally determined differential proton-proton invariant mass

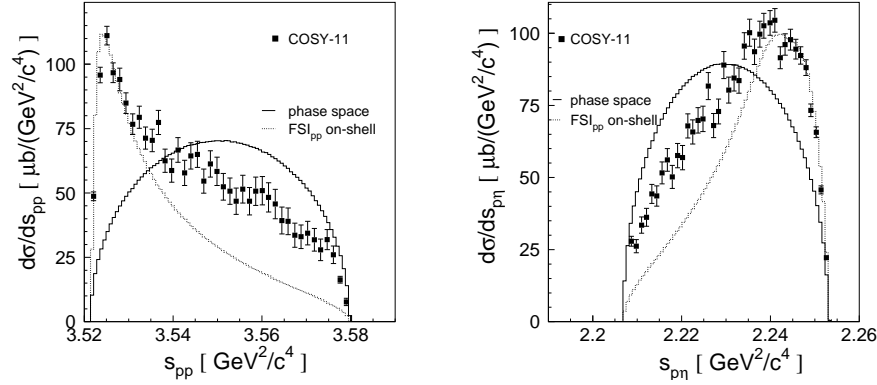


**FIGURE 2.** Distributions of the square of the proton-proton ( $s_{pp}$ ) (left) and proton- $\eta$  ( $s_{p\eta}$ ) (right) invariant masses determined experimentally for the  $pp \rightarrow pp\eta$  reaction (full squares) [1]. The integrals of the phase space weighted by a square of the proton-proton on-shell scattering amplitude (dotted lines)- $FSI_{pp}$ , have been normalized arbitrarily at small values of  $s_{pp}$ . The expectation under the assumption of the homogeneously populated phase space are shown as thick solid lines.

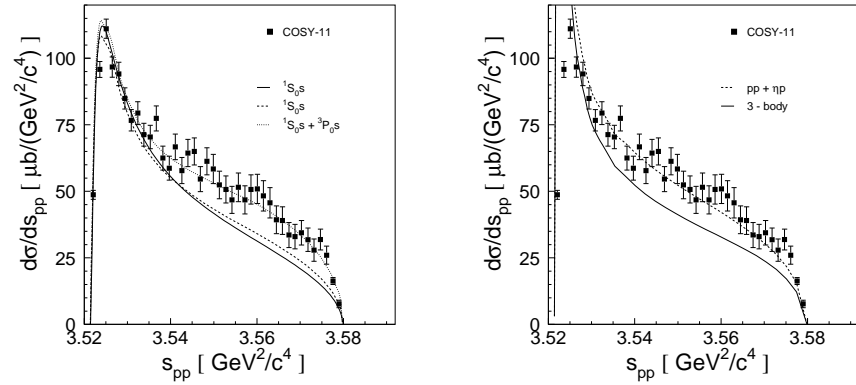


**FIGURE 3.** (left panel) Distribution of the square of the proton-proton ( $s_{pp}$ ) invariant mass determined experimentally for the  $pp \rightarrow pp\eta$  reaction [1]. Solid and dashed lines correspond to the calculations under assumption of  ${}^3P_0 \rightarrow {}^1S_0s$  transition according to the models described in [11] and [9], respectively. The dotted line shows the result of calculations with inclusion of the  ${}^1S_0 \rightarrow {}^3P_0s$  contribution as suggested in [9]. (right panel) The same data as in the left panel but compared to the three-body calculations [10, 12]. The solid line was determined with the rigorous three-body approach. The dashed line depicts the situation if only pairwise interactions ( $pp + p\eta$ ) are allowed.

distribution are presented in the figure 3.

## EXPERIMENT AND DATA ANALYSIS

Using the COSY-11 detection system [13], utilizing a stochastically cooled proton beam and the hydrogen cluster target [14]. The COSY-11 collaboration performed a high statistics measurement of the  $pp \rightarrow pp\eta$  reaction at the beam momentum of

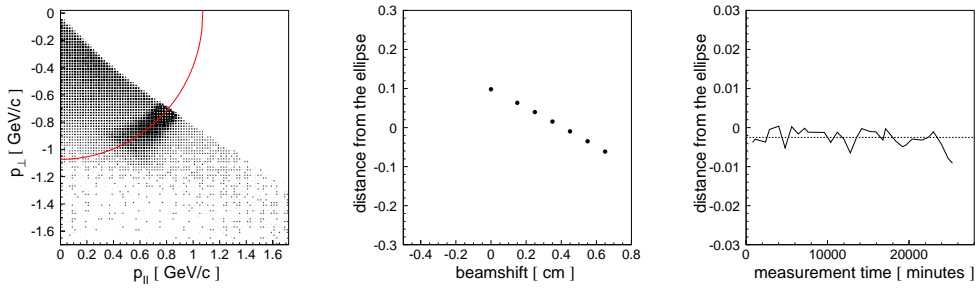


**FIGURE 4.** (left panel) The distribution of the perpendicular  $p_{\perp}$  versus parallel  $p_{\parallel}$  momentum component for the  $pp \rightarrow pp$  elastic scattering determined at the beam momentum of 3.257 GeV/c. The solid line corresponds to the kinematical ellipse. (central panel) The distance between the expected ellipse and the center of experimental distribution on the  $(p_{\perp}, p_{\parallel})$  plot versus a beamshift parameter. (right panel) The deviation of the distance from the kinematical ellipse as a function of the time of measurement. The mean value of the distance from ellipse has been plotted for each of 13 hours intervals.

3.257 GeV/c [1]. The experiment was based on registration of the four-momenta of outgoing protons, whereas the  $\eta'$  meson was identified via the missing mass technique. The missing mass resolution depends on the accuracy of the protons momentum determination which in case of the reconstruction used by COSY-11 group relies on the knowledge of the position of the center of the interaction region. The possible changes of the position where beam crosses target could have significantly influenced the momentum reconstruction and in consequence could worsen the determination of the mass of undetected particle. The center of the beam-target overlap can be determined from the distribution of the momentum of the elastically scattered protons [15]. We applied an analysis of proton-proton elastic scattering for controlling conditions of the beam-target interaction region. The mean value of the distance between the kinematical ellipse and the experimental points (shown in the left panel of figure 4) may be used as a measure of the deviation of the center of the interaction region from its nominal position. In the central panel of the figure 4 the center of the reaction points (beamshift) was expressed with respect to its nominal value. As can be seen, the real position differs by 0.45 cm from the nominal one. In the right panel of figure 4 one can see indication that the beam-target conditions were stable during the course of experiment. Fluctuations seen in that figure originate from statistical error of determination of the mean value of the distance from ellipse. The variations are at the level of  $10^{-3}$  and, as can be inferred from the plot presented in the central panel of the figure 4, correspond to shifts of the center of interactions by less than 0.01 mm. In left panel of the figure 5 we present the preliminary missing mass spectrum, determined for the whole data set, for the  $pp \rightarrow ppX$  reaction measured at the beam momentum of 3.257 GeV/c. In the figure a clear signal is visible with around 17000 events corresponding to the  $pp \rightarrow pp\eta'$  reaction.

Now after introducing the reaction identification, in order to determine the absolute values of cross sections, the luminosity integrated during the measurement time has to be established. One can evaluate it according to a below formula:

$$\frac{\Delta N(\theta^*)}{\Delta \Omega^*(\theta^*)} = \frac{d\sigma^*}{d\Omega^*}(\theta^*) \cdot L, \quad (1)$$

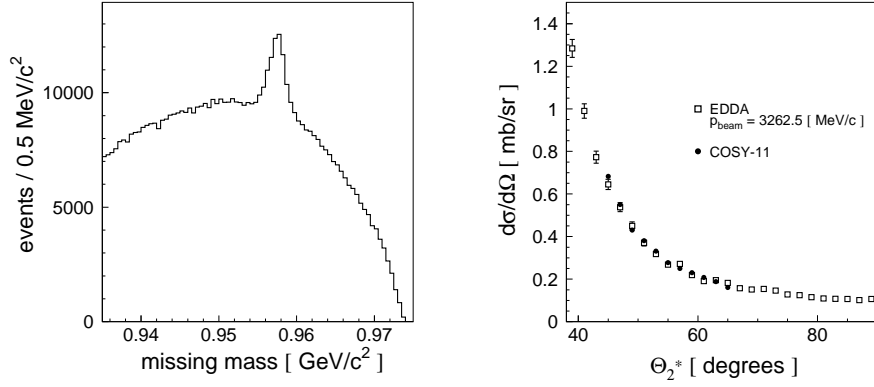


**FIGURE 5.** (left panel) Experimental missing mass spectrum, determined from the whole data set, for the  $pp \rightarrow ppX$  reaction measured at the beam momentum of 3.257 GeV/c. (right panel) Differential cross section for the proton-proton elastic scattering measured at the beam momentum  $p_B = 3.257$  GeV/c, depicted by full circles. Cross section measured by EDDA collaboration is shown by open squares [16].

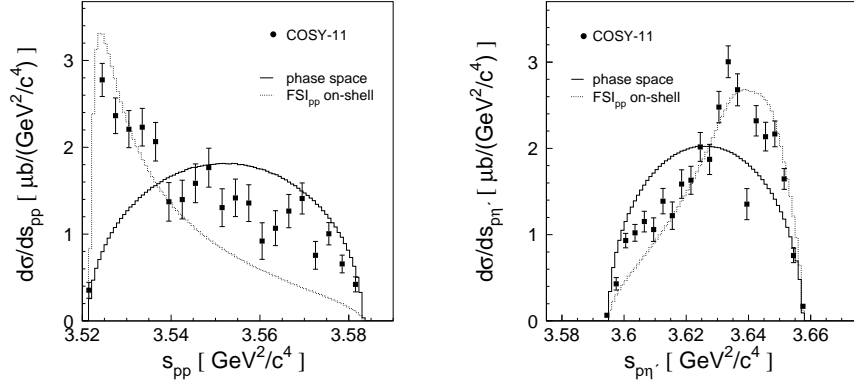


**FIGURE 6.** Preliminary distributions of the square of the proton-proton ( $s_{pp}$ ) (left) and proton- $\eta'$  ( $s_{p\eta'}$ ) (right) invariant masses determined experimentally for the  $pp \rightarrow pp\eta'$  reaction (full circles). The integrals of the phase space weighted by a square of the proton-proton on-shell scattering amplitude (dotted lines)- $FSI_{pp}$ , have been normalized arbitrarily at small values of  $s_{pp}$ . The expectation under the assumption of the homogeneously populated phase space are shown as thick solid lines.

where  $\Delta N(\theta^*)$  indicates number of elastic scattered protons measured at a solid angle  $\Delta\Omega^*$  around the proton emission angle  $\theta^*$  in the center of mass system. The solid angle  $\Delta\Omega^*$  corresponding to a given part of the detection system is calculated as follows:

$$\Delta\Omega^* = \frac{4\pi \cdot N_{accepted}}{2 \cdot N_0} [sr], \quad (2)$$

where  $N_0$  stands for number of proton-proton elastic scattering events simulated and  $N_{accepted}$  denotes number of events seen at the appropriate detector range used to determine  $\Delta N(\theta^*)$ . The center of mass differential cross section  $\frac{d\sigma^*}{d\Omega^*}$  is known from the EDDA experiment [16]. The right panel of the figure 5 indicates the angular distribu-

tion of the differential cross section for elastic proton-proton scattering obtained in the reported here experiment (full circles). The amplitude of that distribution was fitted to the data of the EDDA group including only one free parameter being the integrated luminosity.

The achieved luminosity value  $L = (5.842 \pm 0.072) pb^{-1}$  allowed for the overall normalization of the derived differential cross section as a functions of  $s_{pp}$  and  $s_{p\eta'}$  invariant masses. The preliminary distributions of invariant proton-proton and proton- $\eta'$  masses are presented in the figure 6. The experimental spectra are compared with theoretical calculations. The dotted lines depict calculations where only proton-proton interaction is taken into account and solid lines correspond to a homogeneous phase-space distribution. The homogeneous phase-space distribution deviate strongly from the experimental spectra. It is also easily seen that, the theoretical calculation including proton-proton on-shell interaction do not fit the experimental data at large values of  $s_{pp}$ , similar as it was in case of the  $pp \rightarrow pp\eta$  reaction. The interpretation of presented results is in progress. We hope that presented distributions will help to judge between various interpretations advocated in references [1, 9, 17].

## ACKNOWLEDGMENTS

We acknowledge the support of the European Community-Research Infrastructure Activity under the FP6 programme (Hadron Physics, N4:EtaMesonNet, RII3-CT-2004-506078), the support of the Polish Ministry of Science and Higher Education under the grants No. PB1060/P03/2004/26, 3240/H03/2006/31 and 1202/DFG/2007/03, and the support of the German Research Foundation (DFG).

## REFERENCES

1. P. Moskal *et al.*, Phys. Rev. C **69**, 025203 (2004).
2. F. Balestra *et al.*, Phys. Lett. B **491**, 29 (2000);  
R. Wurzinger *et al.*, Phys. Lett. B **374**, 283 (1996);  
P. Moskal *et al.*, Phys. Rev. Lett. **80** 3202 (1998);  
P. Moskal *et al.*, Phys. Lett. B **474** 416 (2000);  
A. Khoukaz *et al.*, Eur. Phys. J. A **20**, 345 (2004).
3. F. Hibou *et al.*, Phys. Lett. B **438** 41 (1998).
4. E. Chiavassa *et al.*, Phys. Lett. B **322** 270 (1994);  
H. Calén *et al.*, Phys. Rev. Lett. **79** 2642 (1997).
5. A. M. Bergdolt *et al.*, Phys. Rev. D **48**, R2969 (1993).
6. J. Smyrski *et al.*, Phys. Lett. B **474** 182 (2000).
7. H. Calén *et al.*, Phys. Lett. B **366** 39 (1996).
8. A. M. Green, S. Wycech, Phys. Rev. C **55** R2167 (1997).
9. K. Nakayama *et al.*, Phys. Rev. C **68** 045201 (2003).
10. A. Fix, H. Arenhövel, Phys. Rev. C **69** 014001 (2004).
11. V. Baru *et al.*, Phys. Rev. C **67** 024002 (2003).
12. A. Fix, H. Arenhövel, Nucl. Phys. A **697** 277 (2002).
13. S. Brauksiepe *et al.*, Nucl. Instrum. Meth. A **376**, 397 (1996).
14. H. Dombrowski *et al.*, Nucl. Instrum. Meth. A **386**, 228 (1997).
15. P. Moskal *et al.*, Nucl. Instr. & Meth. A **466** 448 (2001).
16. D. Albers *et al.*, Phys. Rev. Lett. **78** 1652 (1997).
17. A. Deloff, Phys. Rev. C **69** 035206 (2004).